JACS
JOURNAL OF THE AMERICAN CHEMICAL SOCIETY

Communication

pubs.acs.org/JACS

Azaboradibenzo[6]helicene: Carrier Inversion Induced by Helical Homochirality

Takuji Hatakeyama,*[,†,‡] Sigma Hashimoto,[†] Tsuyoshi Oba,[†] and Masaharu Nakamura*[,†]

[†]International Research Center for Elements Science (IRCELS), Institute for Chemical Research (ICR), Kyoto University, Uji, Kyoto 611-0011, Japan

[‡]PRESTO, Japan Science and Technology Agency (JST), Kawaguchi-shi, Saitama 332-0012, Japan

Supporting Information

ABSTRACT: Azaboradibenzo[6]helicene, a new semiconductor material possessing helical chirality, has been synthesized via a tandem bora-Friedel–Crafts-type reaction. Unprecedented carrier inversion between the racemate (displaying p-type semiconductivity) and the single enantiomer (displaying n-type semiconductivity) was observed and can be explained by changes in the molecular packing induced by helical homochirality.

Helicenes, nonplanar screw-shaped polycyclic aromatic compounds consisting of ortho-fused aromatic rings, have attracted considerable attention because of their inherent chirality.[1] Recently, the self-assembly of helicenes via unique $\pi-\pi$ stacking interactions in solution as well as in crystals has been studied extensively, since these aggregates display intriguing properties such as liquid crystallinity,[2] nonlinear optical susceptibility,[3] and circularly polarized luminescence.[4] To date, however, the electrical properties of these aggregates (e.g., charge mobility) have not been investigated well,[5] even though the $\pi-\pi$ stacking interactions are expected to facilitate charge transport. Herein we report the synthesis of azaboradibenzo[6]helicene (**A**) via a tandem bora-Friedel–Crafts-type reaction.[6] Charge mobility measurements based on the time-of-flight (TOF) method suggested that the racemate and single enantiomer of **A** are p- and n-type semiconductors, respectively. This unprecedented carrier inversion can be explained by changes in the packing structure of the respective hetero- and homochiral crystals of **A**, as revealed by calculation of the electronic coupling.[7]

Scheme 1 summarizes the synthesis of **A**. 1-Bromo-2-phenylnaphthalene (**1**), prepared in two steps from commercially available 1-bromonaphthalen-2-ol,[8] was coupled with lithium amide in the presence of tris(dibenzylideneacetone)-dipalladium(0) [$Pd_2(dba)_3$] and 2-dicyclohexylphosphino-2′,6′-dimethoxybiphenyl (SPhos) to give diarylamine **2** in 74% yield. Borylation of **2** by treatment with BuLi and BCl_3 and the subsequent tandem bora-Friedel–Crafts-type reaction with $AlCl_3$ and 2,2,6,6-tetramethylpiperidine afforded the racemate of **A** (*rac*-**A**) in 68% yield.

The helical structure of *rac*-**A** was determined to be C_2-symmetric by X-ray crystallography (Figure 1a). The B–N bond length [1.448(3) Å] is similar to that in typical B–N aromatics (1.45–1.47 Å), indicating its strong π interactions.[9] Furthermore, the lengths of the B–C1(C1′) and N–C2(C2′) bonds are 1.5527(19) and 1.425(2), respectively, indicating that they are single bonds. These observations, together with the highly distorted BNC_4 ring structure [B–N–C4(C4′)–C3(C3′) dihedral angle = 21.66°] reveal the low aromaticity of the BNC_4 rings, which is consistent with the relatively small nucleus-independent chemical shift [NICS(1)] value of −1.8 (Figure 1b).[10,11] In contrast, the surrounding C_6 rings are nearly planar and show large NICS(1) values. Notably, molecular orbital (MO) calculations[10] indicated that the π conjugation is spread over the entire molecule despite the large distortion induced by the BNC_4 rings (Figure 1c).

Scheme 1. Synthesis of Azaboradibenzo[6]helicene (A)

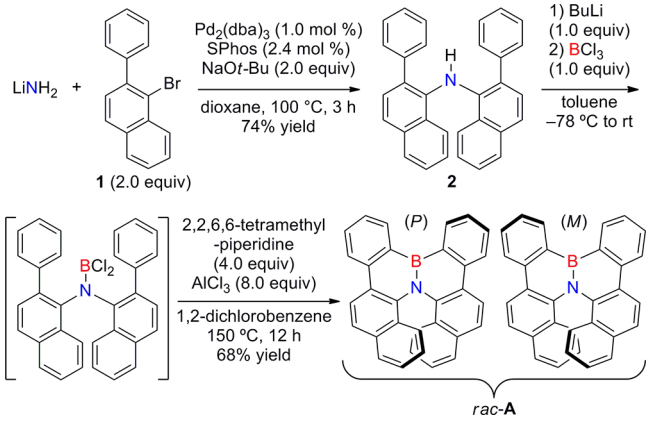

The unique packing structure of the heterochiral crystal is shown in Figure 1d,e. The molecules are stacked in a head-to-tail array with CH–π distances of 2.9–3.3 Å. Each array is formed from a single enantiomer, resulting in alternating right-handed (*P*-helical, shown in blue) and left-handed (*M*-helical, shown in pink) configurations that are arranged in a face-to-face fashion ($\pi-\pi$ distance = 3.4–3.6 Å), while the local dipole moments of the B–N bonds cancel each other.

Optical resolution of *rac*-**A** into enantiopure (*P*)-**A** and (*M*)-**A** was carried out by chiral HPLC on a DAICEL CHIRALPAK IA-3 column (eluent: *n*-hexane/CH_2Cl_2).[12] The absolute configuration of enantiopure **A** in each fraction was determined by X-ray crystallographic analysis of the dibromo derivative of (*P*)-**A**,[13] while the structure of enantiopure (*P*)-**A** was determined by X-ray crystallography (Figure 2). The molecular

Received: October 20, 2012

   dx.doi.org/10.1021/ja310372f | J. Am. Chem. Soc. XXXX, XXX, XXX–XXX

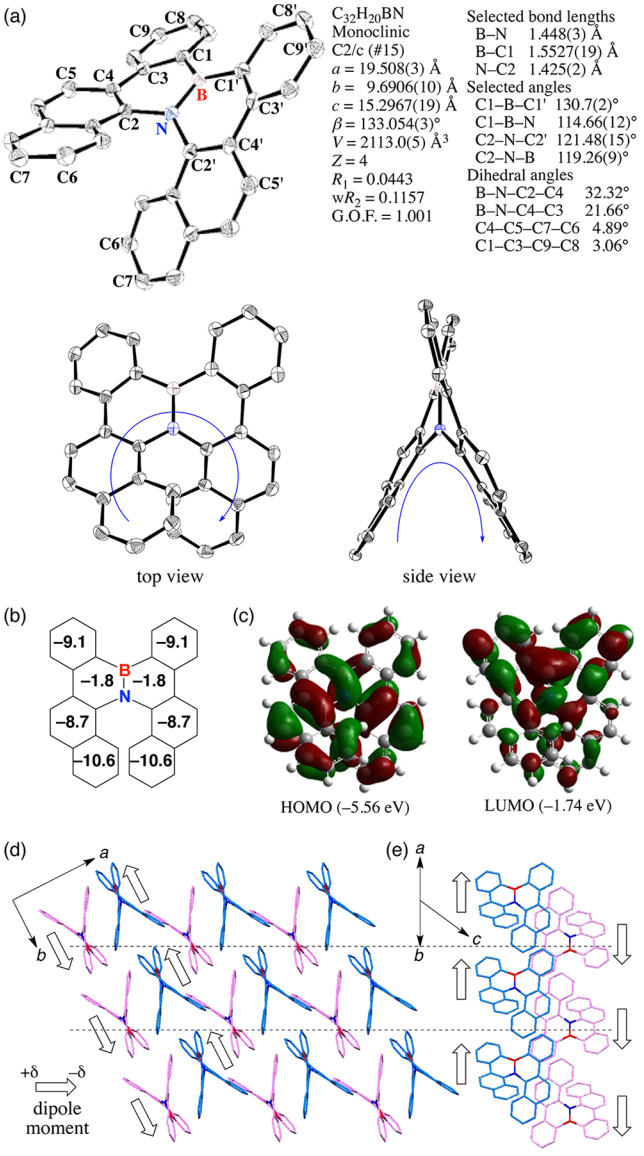

Figure 1. (a) ORTEP drawing and (d, e) packing structure of *rac*-**A** obtained by X-ray crystal analysis. Thermal ellipsoids are shown at 50% probability. H atoms have been omitted for clarity. The *P* enantiomer is shown in blue and the *M* enantiomer in pink. (b) NICS(1) values and (c) the Kohn–Sham highest-occupied MO (HOMO) and lowest unoccupied MO (LUMO) of (*P*)-**A**.

structure of (*P*)-**A** in the homochiral crystal (Figure 2a) is C_2-symmetric, and the bond lengths and angles are almost identical to those found in the heterochiral crystal (Figure 1a). On the other hand, the packing structure of the homochiral crystal differs significantly from that of the heterochiral crystal, as a one-dimensional columnar alignment along the *c* axis was observed (Figure 2b).[14] Interestingly, the molecules in neighboring columns are arranged parallel to each other and show a rotation of 120° with each layer (Figure 2c). As a result, the local dipole moments, which run perpendicular to the *c* axis, are offset every third layer.

Since the enantiopurity of (*P*)-**A** did not decrease upon heating (not even at 275 °C),[15] we prepared films of *rac*-**A** and (*P*)-**A** with thicknesses of 8.2 and 6.7 μm, respectively, by vacuum deposition at 5.0 × 10^{-3} Pa for use in TOF measurements.[8] The carrier-transport properties of the films

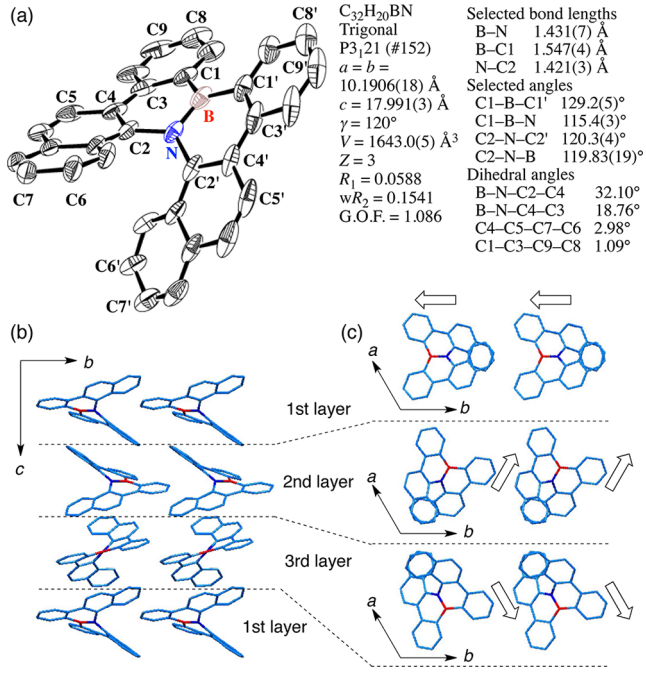

Figure 2. (a) ORTEP drawing and (b, c) packing structure of (*P*)-**A**. Thermal ellipsoids are shown at 30% probability. H atoms have been omitted for clarity.

were then evaluated at room temperature using electric fields of 5.0 × 10^5 and 5.2 × 10^5 V cm^{-1}, respectively. It was found that *rac*-**A** showed high hole mobility (μ_h = 4.6 × 10^{-4} cm^2 V^{-1} s^{-1}),[16] but no transient photocurrent was detected in electron mobility measurements (Table 1). Interestingly, the enantiopure (*P*)-**A** did show higher electron mobility (μ_e = 4.5 × 10^{-3} cm^2 V^{-1} s^{-1}) than hole mobility (μ_h = 7.9 × 10^{-4} cm^2 V^{-1} s^{-1}).[16] Since the corresponding physical properties of the vacuum-deposited films, such as ionization potential (IP) and electron affinity (EA),[17] were almost identical, we speculated that the carrier inversion could be caused by the distinct orientation of (*P*)-**A** in the homochiral film.

Table 1. Electronic Properties of Amorphous Films of *rac*-A and (*P*)-A

	μ_h[a]		μ_e[b]	I_p[c]	E_a[d]
rac-**A**	4.6 × 10^{-4}	>>	—[e]	5.54	2.55
(*P*)-**A**	7.9 × 10^{-4}	<<	4.5 × 10^{-3}	5.55	2.55

[a]Hole mobility (cm^2 V^{-1} s^{-1}). [b]Electron mobility (cm^2 V^{-1} s^{-1}). [c]Ionization potential (eV). [d]Electron affinity (eV). [e]Transient photocurrent was not detected.

To gain deeper insight into the carrier-transport properties, the electronic couplings *V* between neighboring molecules in different stacks were calculated[18] from the X-ray crystal structures of *rac*-**A** and (*P*)-**A** (Figure 3). In the heterochiral crystal of *rac*-**A** (Figure 3a), the *P* and *M* enantiomers are arranged in a tightly offset, face-to-face stacking array. The maximum coupling between the HOMOs of neighboring molecules (42.0 meV) was 6 times that of the corresponding LUMOs (7.2 meV). In contrast, in the homochiral crystal of (*P*)-**A** (Figure 3b), the maximum coupling of the HOMOs (30.1 meV) was only two-fifths that of the LUMOs (73.2 meV). These results are in good agreement with the carrier

dx.doi.org/10.1021/ja310372f | J. Am. Chem. Soc. XXXX, XXX, XXX–XXX

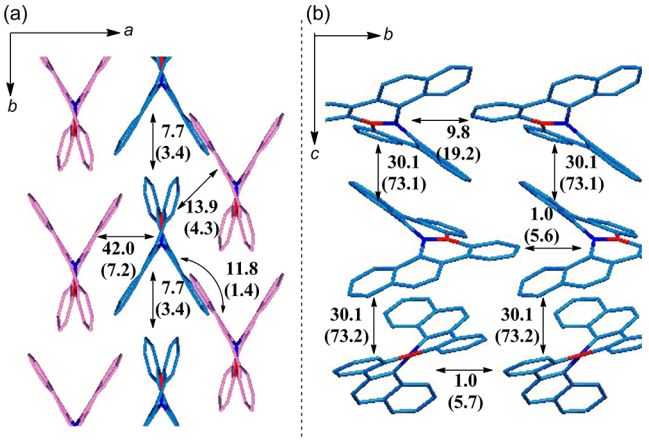

Figure 3. Electronic couplings V (in meV) between HOMOs of neighboring molecules in the X-ray crystal structures of (a) *rac*-**A** (P in blue, M in pink) and (b) (P)-**A**. The electronic couplings between LUMOs are shown in parentheses.

mobilities determined by the TOF method,[18] suggesting the possibility that the molecular orientations in the amorphous films might be similar to those in the crystals.[19]

In summary, we have synthesized azaboradibenzo[6]helicene (**A**) via a tandem bora-Friedel–Crafts-type reaction. Charge mobility measurements by the time-of-flight (TOF) method suggested that the racemate and single enantiomer of **A** are good p- and n-type semiconductors, respectively. This unprecedented carrier inversion can be explained by differences in the packing structures of the hetero- and homochiral crystals of **A**, as revealed by electronic coupling calculations. The results indicate the potential of these chiral organic semiconductors in electronic applications such as bipolar junction transistors and morphology-controlled bulk-heterojunction solar cells.

■ ASSOCIATED CONTENT

Ⓢ Supporting Information

Experimental procedures; characterization, photophysical, electrochemical, and crystallographic data and CIF files for the products; and computational methods and data. This material is available free of charge via the Internet at http://pubs.acs.org.

■ AUTHOR INFORMATION

Corresponding Author

hatake@scl.kyoto-u.ac.jp; masaharu@scl.kyoto-u.ac.jp

Notes

The authors declare no competing financial interest.

■ ACKNOWLEDGMENTS

This research was supported by the PRESTO Program of JST and a Grant-in-Aid for Young Scientists (23685020) from the Ministry of Education, Culture, Sports, Science and Technology (MEXT) of Japan. The study was also supported by the NEXT Program of the Japan Society for the Promotion of Science (JSPS) and the Asahi Glass Foundation. We thank Mr. Toshiaki Ikuta and Dr. Jingping Ni (JNC Petrochemical Corporation) for TOF and IP measurements and Professors Mao Minoura (Kitasato University) and Hikaru Takaya and Takahiro Sasamori (Kyoto University) for their guidance in the X-ray crystallography experiments. For initial investigations, synchrotron X-ray powder diffraction measurements were performed on beamline BL19B2 at SPring-8 with the approval of JASRI (2009B1785, 2010A1721).

■ REFERENCES

(1) Recent reviews: (a) Stary, I.; Stara, I. G.; Alexandrova, Z.; Sehnal, P.; Teply, F.; Saman, D.; Rulisek, L. *Pure Appl. Chem.* **2006**, *78*, 495–499. (b) Collins, S. K.; Vachon, M. P. *Org. Biomol. Chem.* **2006**, *4*, 2518–2524. (c) Rajca, A.; Rajca, S.; Pink, M.; Miyasaka, M. *Synlett* **2007**, 1799–1822. (d) Amemiya, R.; Yamaguchi, M. *Chem. Rec.* **2008**, *8*, 116–127. (e) Dumitrascu, F.; Dumitrescu, D. G.; Aron, I. *ARKIVOC* **2010**, No. 1, 1–32. (f) Jørgensen, K. B. *Molecules* **2010**, *15*, 4334–4358. (g) Shen, Y.; Chen, C.-F. *Chem. Rev.* **2012**, *112*, 1463–1535.

(2) (a) Nuckolls, C.; Katz, T. J. *J. Am. Chem. Soc.* **1998**, *120*, 9541–9544. (b) Vyklicky, L.; Eichhorn, S. H.; Katz, T. J. *Chem. Mater.* **2003**, *15*, 3594–3601. (c) Shcherbina, M. A.; Zeng, X.-B.; Tadjiev, T.; Ungar, G.; Eichhorn, S. H.; Phillips, K. E. S.; Katz, T. J. *Angew. Chem., Int. Ed.* **2009**, *48*, 7837–7840.

(3) (a) Verbiest, T.; Elshocht, S. V.; Kauranen, M.; Hellemans, L.; Snauwaert, J.; Nuckolls, C.; Katz, T. J.; Persoons, A. *Science* **1998**, *282*, 913–915. (b) Verbiest, T.; Elshocht, S. V.; Persoons, A.; Nuckolls, C.; Phillips, K. E.; Katz, T. J. *Langmuir* **2001**, *17*, 4685–46867. (c) Verbiest, T.; Sionke, S.; Persoons, A.; Vyklicky, L.; Katz, T. J. *Angew. Chem., Int. Ed.* **2002**, *41*, 3882–3884.

(4) (a) Field, J. E.; Muller, G.; Riehl, J. P.; Venkataraman, D. *J. Am. Chem. Soc.* **2003**, *125*, 11808–11809. (b) Kaseyama, T.; Furumi, S.; Zhang, X.; Tanaka, K.; Takeuchi, M. *Angew. Chem., Int. Ed.* **2011**, *50*, 3684–3687.

(5) (a) Kim, C.; Marks, T. J.; Facchetti, A.; Schiavo, M.; Bossi, A.; Maiorana, S.; Licandro, E.; Todescato, F.; Toffanin, S.; Muccini, M.; Graiff, C.; Tiripicchio, A. *Org. Electron.* **2009**, *10*, 1511–1520. (b) Sahasithiwat, S.; Mophuang, T.; Menbangpung, L.; Kamtonwong, S.; Sooksimuang, T. *Synth. Met.* **2010**, *160*, 1148–1152.

(6) Hatakeyama, T.; Hashimoto, S.; Seki, S.; Nakamura, M. *J. Am. Chem. Soc.* **2011**, *133*, 18614–18617.

(7) (a) Velde, G. T.; Bickelhaupt, F. M.; Baerends, E. J.; Fonseca Guerra, C.; Gisbergen, S. J. A. V.; Snijders, J. G.; Ziegler, T. *J. Comput. Chem.* **2001**, *22*, 931–967. (b) Senthilkumar, K.; Grozema, F. C.; Bickelhaupt, F. M.; Siebbeles, L. D. A. *J. Chem. Phys.* **2003**, *119*, 9809–9817. (c) Wen, S.-H.; Li, A.; Song, J.; Deng, W.-Q.; Han, K.-L.; Goddard, W. A., III. *J. Phys. Chem. B* **2009**, *113*, 8813–8819.

(8) See the Supporting Information for details.

(9) Reviews: (a) Liu, Z.; Marder, T. B. *Angew. Chem., Int. Ed.* **2008**, *47*, 242–244. (b) Bosdet, M. J. D.; Piers, W. E. *Can. J. Chem.* **2009**, *87*, 8–29. (c) Ashe, A. J., III. *Organometallics* **2009**, *28*, 4236–4248. (d) Campbell, P. G.; Marwitz, A. J. V.; Liu, S.-Y. *Angew. Chem., Int. Ed.* **2012**, *51*, 6074–6092.

(10) DFT calculations, including NICS analyses, were performed at the B3LYP/6-311+G(d,p)//B3LYP/6-31G(d) level as implemented in the Gaussian 09 program. See the Supporting Information for details.

(11) Reported NICS(1) values for the planar BNC_4 rings in BN-substituted aromatics are −4.6 and −6.3 ppm. See: Bosdet, M. J. D.; Jaska, C. A.; Piers, W. E.; Sorensen, T. S.; Parvez, M. *Org. Lett.* **2007**, *9*, 1395–1398.

(12) UV–vis, fluorescence, and CD measurements were performed for *rac*-**A** and enantiopure (P)-**A** and (M)-**A**. See the Supporting Information for details.

(13) Dibromination of **A** took place selectively at the para position of the aniline moiety in the presence of 2 equiv of *N*-bromosuccinimide. See the Supporting Information for details.

(14) One-dimensional columnar alignment of helicenes: (a) Murguly, E.; McDonald, R.; Branda, N. R. *Org. Lett.* **2000**, *2*, 3169–3172. (b) Caronna, T.; Sinisi, R.; Catellani, M.; Malpezzi, L.; Meille, S. V.; Mele, A. *Chem. Commun.* **2000**, 1139–1140. (c) Miyasaka, M.; Rajca, A.; Pink, M.; Rajca, S. *J. Am. Chem. Soc.* **2005**, *127*, 13806–13807. (d) Nakano, K.; Oyama, H.; Nishimura, Y.; Nakasako, S.; Nozaki, K. *Angew. Chem., Int. Ed.* **2012**, *51*, 695–699.

(15) The calculated racemization barrier [$\Delta H^{\ddagger}$ at the B3LYP/6-31G(d) level] is 42.0 kcal mol^{-1}, which is consistent with the experimental results and considerably higher than that of the [6] helicene (35.2 kcal mol^{-1}). See: Grimme, S.; Peyerimhoff, S. D. *Chem. Phys.* **1996**, *204*, 411−417.

(16) The charge mobilities are comparable to those in representative organic semiconductors (measured by the TOF method), such as α-naphthylphenylbiphenyldiamine (α-NPD, $\mu_h = 7 \times 10^{-4}$ cm^2 V^{-1} s^{-1}), 1,3,5-tris(phenyl-2-benzimidazolyl)benzene (TPBI, $\mu_e = 9 \times 10^{-5}$ cm^2 V^{-1} s^{-1}), and 4,4′-*N*,*N*′-dicarbazolebiphenyl (CBP, $\mu_h = 2 \times 10^{-3}$ cm^2 V^{-1} s^{-1}, $\mu_e = 1 \times 10^{-3}$ cm^2 V^{-1} s^{-1}). See: (a) Hung, W.-Y.; Ke, T.-H.; Lin, Y.-T.; Wu, C.-C.; Hung, T.-H.; Chao, T.-C.; Wong, K.-T.; Wu, C.-I. *Appl. Phys. Lett.* **2006**, *88*, No. 064102. (b) Li, C.; Duan, L.; Sun, Y.; Li, H.; Qiu, Y. *J. Phys. Chem. C* **2012**, *116*, 19748−19754.

(17) IPs were measured by photoelectron spectroscopy in air (PESA) using an AC-1 system (RIKEN KEIKI Co., Ltd.). EAs were estimated from the IPs and UV−vis absorption-edge wavelengths.

(18) Electronic coupling (V) calculations were performed using the PW91 hybrid functional with the DZP basis set as implemented in the ADF2010 program. The electron-hopping rate (W) is proportional to V^2 on the basis of the Marcus−Hush theory. See ref 6 and citations therein.

(19) Molecular orientation in vacuum-deposited amorphous films: Yokoyama, D. *J. Mater. Chem.* **2011**, *21*, 19187−19202 and citations therein.